Appl Biochem Biotechnol (2010) 160:280–297
DOI 10.1007/s12010-008-8512-9

Effect and Modeling of Glucose Inhibition and In Situ Glucose Removal During Enzymatic Hydrolysis of Pretreated Wheat Straw

Pavle Andrić · Anne S. Meyer · Peter A. Jensen · Kim Dam-Johansen

Received: 14 October 2008 / Accepted: 24 December 2008 /
Published online: 23 January 2009

Abstract The enzymatic hydrolysis of lignocellulosic biomass is known to be product-inhibited by glucose. In this study, the effects on cellulolytic glucose yields of glucose inhibition and in situ glucose removal were examined and modeled during extended treatment of heat-pretreated wheat straw with the cellulolytic enzyme system, Celluclast® 1.5 L, from *Trichoderma reesei*, supplemented with a β-glucosidase, Novozym® 188, from *Aspergillus niger*. Addition of glucose (0–40 g/L) significantly decreased the enzyme-catalyzed glucose formation rates and final glucose yields, in a dose-dependent manner, during 96 h of reaction. When glucose was removed by dialysis during the enzymatic hydrolysis, the cellulose conversion rates and glucose yields increased. In fact, with dialytic in situ glucose removal, the rate of enzyme-catalyzed glucose release during 48–72 h of reaction recovered from 20–40% to become ≈70% of the rate recorded during 6–24 h of reaction. Although Michaelis–Menten kinetics do not suffice to model the kinetics of the complex multi-enzymatic degradation of cellulose, the data for the glucose inhibition were surprisingly well described by simple Michaelis–Menten inhibition models without great significance of the inhibition mechanism. Moreover, the experimental in situ removal of glucose could be simulated by a Michaelis–Menten inhibition model. The data provide an important base for design of novel reactors and operating regimes which include continuous product removal during enzymatic hydrolysis of lignocellulose.

Keywords Cellulases · Lignocellulose · Product inhibition · Product removal · Reactor design

Introduction

The conversion of cellulosic biomass into bioethanol is currently studied worldwide to develop CO_2-neutral biofuel alternatives to fossil fuels. One of the first prerequisites in such

P. Andrić · A. S. Meyer (✉) · P. A. Jensen · K. Dam-Johansen
Department of Chemical and Biochemical Engineering, Technical University of Denmark,
DK-2800 Kgs Lyngby, Denmark
e-mail: am@kt.dtu.dk

ethanol production is the efficient generation of a fermentable hydrolysate, rich in glucose, from the cellulose present in the biomass feedstock. The enzyme-catalyzed degradation of lignocellulose for bioethanol production is particularly well described for the cellulases produced by the fungus *Trichoderma reesei* [1–3], and the *T. reesei* cellulases are now considered "the industry standard" for enzymatic lignocellulose hydrolysis [1]. *T. reesei* secretes high amounts of enzymes, up to 40 g/L, including at least five different endoglucanases and two types of cellobiohydrolase activities, as well as a number of xylanases and at least one β-xylosidase enzyme [4–6]. *T. reesei* also produces a β-glucosidase, but since this enzyme activity is bound to the mycelium, it is not recovered efficiently during industrial cellulase production and needs to be supplemented. The workability of a *T. reesei* production strain expressing a β-glucosidase from *Aspergillus oryzae* has recently been demonstrated [1], but most application studies evaluating the enzymatic degradation of lignocellulose by *T. reesei* cellulases have up until now used exogenous supplementation of a β-glucosidase activity. Particularly, many studies have employed addition of a β-glucosidase preparation from *Aspergillus niger*, Novozym® 188, to the commercial *T. reesei* product, Celluclast® 1.5 L (both preparations manufactured by Novozymes A/S) to, e.g., assess the impact of different pretreatments, enzyme reaction conditions, inhibitors, etc., on glucose yields during enzymatic lignocellulose hydrolysis [7–10].

Cellobiose and glucose are known to be inhibitory to the action of cellulolytic enzymes, including those from *T. reesei* and the β-glucosidase from *A. niger* [10]. Glucose thus directly inhibits β-glucosidase, but also cellobiohydrolases and endoglucanases (Fig. 1), while cellobiose directly inhibits cellobiohydrolases and endoglucanases (Fig. 1). Via the inhibition of β-glucosidase, which results in accumulation of cellobiose, glucose in turn indirectly inhibits cellobiohydrolases and endoglucanases. In addition, cellulose and cellobiose exert substrate inhibition on cellobiohydrolases and endoglucanases and β-glucosidase, respectively (Fig. 1). β-Glucosidase from *A. niger* [11] as well as the *T. reesei* β-glucosidase [12] can moreover catalyze a reverse reaction in which glucose molecules via transglycosylation are transferred to glucose or cellobiose to yield different di-, tri-, and oligosaccharides.

Product inhibition of (ligno)cellulose degrading enzymes is one of several major factors that decrease the cellulolytic hydrolysis rate and product yields [13, 14]. Quantitative knowledge about the glucose product inhibition is thus paramount for proper selection, design, simulation, optimization and scale-up of enzymatic hydrolysis reactors for lignocellulose conversion [15–18]. This is particularly important in separate hydrolysis and fermentation regimes in which the glucose accumulates as the reaction is advancing and

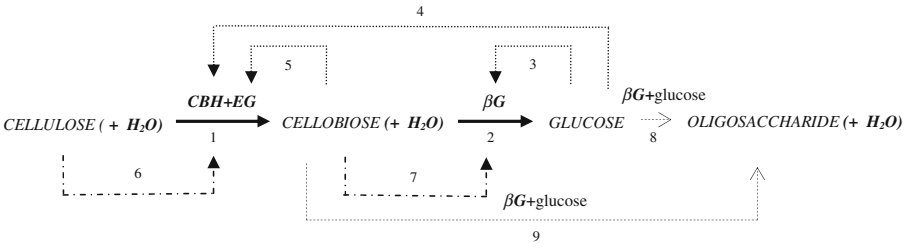

Fig. 1 Overview of the major kinetic pathways for cellulolytic enzymes: *solid line*, the main reaction (*1*, *2*); *dotted line*, product inhibition (*3*) [36], (*4*) [22], (*5*) [16]; *dashed-dotted line*, substrate inhibition (*6*) [40, 41], (*7*) [23]; *dashed line*, transglycosylation (*8*, *9*) [11, 12]. *CBH* cellobiohydrolase, *EG* endoglucanase, *βG* β-glucosidase

less significant in the simultaneous hydrolysis and fermentation setup in which the glucose level is very low due to its almost instant consumption by the fermenting microorganism.

The renewed interest in the design of alternative and more efficient hydrolysis reactors (than stirred batch), such as reactors with integrated cellulose digestion and inhibitory product removal [19–21], requires quantitative data for the glucose inhibition of the cellulase system. Several reports are available on the glucose inhibition of *T. reesei* cellulase systems acting on pure cellulose [10, 18, 22, 23], but there is a surprising scarcity of quantitative data for glucose inhibition of the cellulolytic degradation on genuine lignocellulose substrates. Xiao et al. [10] observed significant inhibitory effects of glucose-, cellobiose-, and hemicellulose-derived monosaccharides during enzymatic hydrolysis of Avicel and acetic-acid-pretreated softwood using the Celluclast®–Novozym® 188 cellulase system. They also observed a rate-increasing effect of product removal via intermission after 24 and 48 h of hydrolysis, but did not attempt to model the events [10]. Frenneson et al. [24] developed an empirical model to describe the exponential decrease in the rate of degradation of hammer-milled and alkali-pretreated sallow caused by product inhibition by glucose during Celluclast®–Novozym® 188 treatment.

The present study was undertaken to investigate the significance of glucose inhibition and in situ glucose removal, respectively, during cellulolytic degradation of hydrothermally pretreated wheat straw as catalyzed by the Celluclast® 1.5 L–Novozym® 188 system during extended reaction (4 days). Furthermore, since the application of less complex kinetic equations to model the formation of glucose in the hydrolysis of insoluble cellulose is a huge advantage [15], another objective of this study was to examine the workability of relatively simple kinetic models to describe the enzymatic progress curves during glucose inhibition and during in situ removal of glucose.

Materials and Methods

Chemicals

D-(+)-Glucose (anhydrous) 99.5% was purchased from Merck (Darmstadt, Germany) and tetracycline ≥98% from Sigma-Aldrich Chemical Co. (St. Louis, MO, USA).

Cellulolytic Enzymes

Celluclast® 1.5 L from *T. reesei* and Novozym® 188 from *A. niger* were both donated by Novozymes A/S (Bagsværd, Denmark). The Celluclast® 1.5-L preparation had a filter paper unit (FPU) activity of 47 FPU/mL as measured by the FPU assay of the US National Renewable Energy Laboratory [25]. Novozym® 188 had an activity of 246 CBU/g of preparation; CBU designates cellobiase units as determined by glucose production on cellobiose at 40 °C, pH 5 (provided by Novozymes A/S).

Lignocellulosic Substrate

The lignocellulosic material used in this study was wheat straw pretreated in the demonstration plant Fynsværket (Odense, Denmark) operated by DONG Energy A/S (Fredericia, Denmark). Whole bales of wheat straw were treated by a hot water extraction process in a three-step counter-current reactor (60 °C, 15 min; 180 °C, 10 min; 195 °C, 3 min, at ≈16% dry matter by weight) that extracted a hemicellulose-rich liquid fraction

(which was removed after the first step) and left a solid fraction rich in cellulose and lignin [8]. The latter, solid fraction, referred to as pretreated straw, was the lignocellulosic substrate material used in the present study. This pretreated substrate material, 28±4% dry matter by weight (DM, *w*/*w*), was stored at −18 °C until use. The compositional carbohydrate analysis (arabinose 5.8±1.0, xylose 7.1±0.6, and glucose 48±7.8% DM, *w*/*w*) [8] was done according to the NREL standard methodology [26]. Prior to the enzymatic hydrolysis experiments, the substrate was ground using a cutting mill (Retsch SM 2000, Haan, Germany) to pass through a mesh size of 4 mm.

Enzymatic Hydrolysis

Aliquots of the ground pretreated wheat straw were diluted to 2% DM (*w*/*w*) in 1 M sodium citrate buffer with tetracycline (final tetracycline concentration 0.4%, *v*/*v*) [27], the Celluclast® 1.5 L and Novozym® 188 were added (weight ratio 4:1), and the enzymatic hydrolysis reactions were accomplished for 96 h at a reaction volume of 50 mL, at pH 5 and 50 °C. In all experiments, the enzymatic dosage of Celluclast® 1.5 L was 8 FPU per gram substrate DM and that of Novozym® 188 was 13 CBU per gram substrate DM, equivalent to 0.205 g Celluclast® 1.5L/g substrate DM and 0.054 g Novozym® 188/g substrate DM, respectively.

The hydrolysis reaction temperature was controlled by keeping the reaction vessels in a water bath Julabo Open Heating Bath Circulator EH-33 (JULABO Labortechnik GmbH, Seelbach, Germany). Agitation was done using triangular magnetic stirrers at 350 rpm and controlled by a magnetic stirrer system (Telesystem 15.20, H+P Labortechnik, Oberschleiβheim, Germany) which was immersed in the water bath. In the glucose inhibition studies, four levels of glucose were added to reach the following glucose concentrations in the reaction vessels, respectively (prior to addition of the enzymes), 0, 10, 20, and 40 g glucose per liter.

Samples, in duplicates, were collected after 1, 2, 4, 6, 24, 48, 72, and 96 h and heated immediately at 100 °C for 10 min to halt the enzymatic reactions. The samples were then cooled, centrifuged for 10 min at 10 °C and max. 24,000×*g*, and filtered (0.2 μm single-use PTFE filters) and the levels of glucose determined by high-performance anion exchange chromatography (HPAEC).

Product Analysis by HPAEC

Separation and quantification of glucose in the hydrolysates were accomplished by HPAEC analysis using a Dionex® BioLC system (Dionex Corp., Sunnyvale, CA, USA) consisting of GS50 gradients pumps, an ED50 electrochemical detector, and an AS50 chromatography compartment coupled to an AS50 autosampler. Prior to injection, the samples were appropriately diluted with doubly deionized water. The samples (10 μL) were eluted isocratically with 2.5 mM NaOH at a flow rate of 0.5 mL/min through a CarboPac™ PA20 (3×150 mm) analytical column (Dionex Corp.) [28]. The data were collected on a PC and analyzed by means of Chromeleon 6.60 Sp2 Build 1472 software (Dionex Corp.). Glucose quantification was done using an external standard.

Glucose Removal by Different Methods

The removal of glucose during enzymatic hydrolysis was performed using a 2% substrate DM (*w*/*w*) reaction mixture (enzymatic hydrolysis conditions as described above) under the

following three different regimes (Fig. 2): (1) removal of a liquid portion by filtration after 24 h and replenishment with fresh buffer; (2) removal of a liquid portion by filtration after 24 h and replenishment with fresh buffer and enzymes; and (3) in situ removal of glucose via a Spectra/Por® 6 dialysis membrane during 24–48 h of reaction. In addition, two control experiments were done (each in duplicate): in the first, the reactor was magnetically stirred as described above, and in the second, no stirring was done except when the reactor was shaken manually prior to sampling.

The membrane cutoff of the dialysis membrane, 1 kDa, was selected on the basis of the molecular weights of glucose (0.18 kDa) and cellulases (≈5–90 kDa). The dialysis membrane Spectra/Por® 6 [Spectrum Laboratories Inc., Rancho Dominguez, CA, USA; diameter 24 mm, flat width 38 mm, volume/length 4.6 mL/cm, membrane cutoff 1 kDa (≈1 nm)] was stored in 0.1% sodium azide solution, soaked for 30 min, and washed in distilled water prior to use. This membrane was chosen because of its robustness as stated by the manufacturer (Spectrum Laboratories Inc.). Glucose was removed from the hydrolysis reactor across the membrane into the collection vessel, which was filled with 2 L of dialysate solution (1 M sodium citrate buffer, pH 5) and magnetically stirred (Fig. 2). Samples were taken both from the reactor and the dialysate solution.

Kinetic Modeling

In the inhibition studies with glucose addition, four types of Michaelis/Menten-based models, including the classical (uninhibited) Michaelis–Menten equation, and three inhibition models, competitive, non-competitive, and uncompetitive, were solved analytically and numerically to obtain integrated rate equations (Table 1) and to assess the model quality. The apparent kinetic parameters were estimated by a nonlinear least-squares method, while the confidence intervals and uncertainty estimates were determined using linear error propagation [29]. The initial parameter guesses were: k_{cat}=10 h^{-1}, K_M=1 mM, K_{IG}=10 mM, while the constants were S_0=0.136 mM, E_0=0.01 mM, n=450, of which the last was determined in an independent optimization study (data not shown). Each model

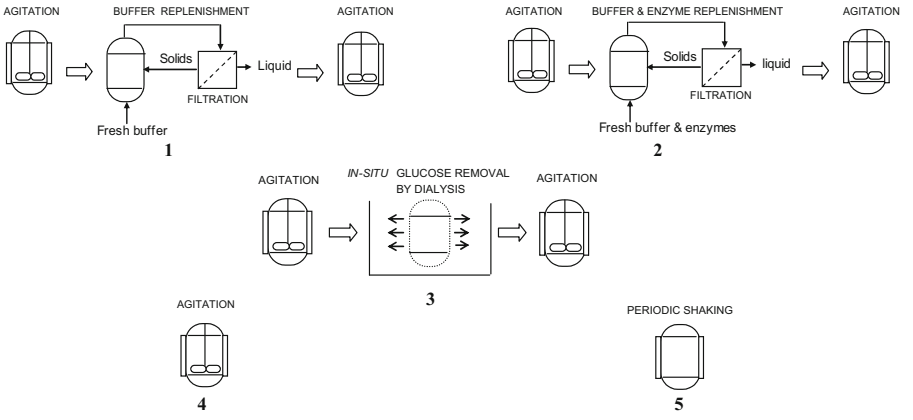

Fig. 2 Schematic representation of glucose removal experiments by: (1) filtration and buffer replenishment (agitated from 0–24 h, filtered for 15 min, liquid portion replaced with fresh buffer, and agitated up to 96 h); (2) filtration and buffer and enzyme replenishment (agitated from 0–24 h, filtered for 15 min, liquid portion replaced with fresh buffer and enzymes, and agitated up to 96 h); (3) dialysis membrane (in situ; agitated from 0–24 h, dialysis from 24–48 h, and agitated for up to 96 h). Experiments 4 and 5 were controls (no glucose removal), with constant agitation and intermittent shaking when samples were taken, respectively

Table 1 Modeling hydrolysis of pretreated wheat straw by Celluclast® 1.5 L and Novozym® 188 in the presence of initially added glucose (0–40 g/L).

Model no.	Inhibition type	Mechanism	Reaction rate, v (M s^{-1})	Integrated reaction time expressions (s)
1	No inhibition	$E+S\underset{k_{-1}}{\overset{k_1}{\rightleftarrows}}ES\xrightarrow{k_2}E+nG$	$\frac{k_{cat}E_0S}{K_M+S}$	$\frac{1}{k_{cat}E_0}\left(-K_M\ln\left(1-\frac{c(G-G_0)}{S_0}\right)+c(G-G_0)\right)$
2	Competitive	$E+S\underset{k_{-1}}{\overset{k_1}{\rightleftarrows}}ES\xrightarrow{k_2}E+nG$ $E+G\underset{k_{G-1}}{\overset{k_{G1}}{\rightleftarrows}}EG$	$\frac{k_{cat}E_0S}{K_M\left(1+\frac{G}{K_{IG}}\right)+S}$	$\frac{1}{k_{cat}E_0}\left(-\left(K_M+\frac{K_M}{K_{IG}c}(cG_0+S_0)\right)\ln\left(1-\frac{c(G-G_0)}{S_0}\right)+\left(1-\frac{K_M}{K_{IG}c}\right)c(G-G_0)\right)$
3	Non-competitive	$E+S\underset{k_{-1}}{\overset{k_1}{\rightleftarrows}}ES\xrightarrow{k_2}E+nG$ $E+G\underset{k_{G-1}}{\overset{k_{G1}}{\rightleftarrows}}EG$ $ES+G\underset{k_{G-1}}{\overset{k_{G1}}{\rightleftarrows}}ESG$	$\frac{k_{cat}E_0S}{(K_M+S)\left(1+\frac{G}{K_{IG}}\right)}$	$\frac{1}{k_{cat}E_0}\left(-\left(K_M+\frac{K_M}{K_{IG}c}(cG_0+S_0)\right)\ln\left(1-\frac{c(G-G_0)}{S_0}\right)+\left(1-\frac{K_M}{K_{IG}c}\right)c(G-G_0)+\frac{c}{2K_{IG}}\left(G^2-G_0^2\right)\right)$
4	Un-competitive	$E+S\underset{k_{-1}}{\overset{k_1}{\rightleftarrows}}ES\xrightarrow{k_2}E+nG$ $ES+G\underset{k_{G-1}}{\overset{k_{G1}}{\rightleftarrows}}ESG$	$\frac{k_{cat}E_0S}{K_M+S\left(1+\frac{G}{K_{IG}}\right)}$	$\frac{1}{k_{cat}E_0}\left(-K_M\ln\left(1-\frac{c(G-G_0)}{S_0}\right)+\left(1+\frac{G_0}{K_{IG}}\right)c(G-G_0)+\frac{c}{2K_{IG}}(G-G_0)^2\right)$

Summary of inhibition types and mechanisms, expressions for reaction rates, and integrated hydrolysis time. Overall reaction was $S+nH_2O\rightarrow nG$; substrate mol balance was given with $S=S_0-\frac{1}{n}(G-G_0)=S_0-c(G-G_0)$ and reaction rate was $v=-\frac{dS}{dt}=\frac{1}{n}\frac{dG}{dt}=c\times r$

was regressed on all available data. The quality assessment of the model prediction of net glucose concentration in the presence of different levels of added glucose was based on estimated parameter values and 95% confidence intervals, as well as on parameter correlation coefficients. For the simulation of glucose removal by dialysis, the optimal parameters determined were used.

Results and Discussion

Glucose Inhibition of Enzymatic Cellulose Hydrolysis: Effect on Yields

Glucose inhibition of the cellulase system consisting of Celluclast® 1.5 L from *T. reesei* and Novozym® 188 from *A. niger* (added in a 4:1 weight ratio) was assessed during enzymatic hydrolysis of hydrothermally pretreated wheat straw reacted at a substrate concentration of 2% (*w*/*w*) DM. The glucose inhibition was studied by addition of different levels of glucose in a concentration range of 0–40 g/L.

The addition of glucose resulted in a significant dose-dependent effect on the total glucose concentration (Fig. 3). The progress curve for the enzymatic hydrolysis without glucose addition (‘0 g/L’, Fig. 3) showed that the glucose concentration increased rapidly during the first 6 h of hydrolysis. In contrast, only a very small increase in glucose concentration with hydrolysis time was seen for the ‘10 g/L’ and the ‘20 g/L’ curves. The ‘40 g/L’ curve even had a slightly negative slope of total glucose concentration during the initial enzymatic reaction (Fig. 3).

Except for the reaction to which 40 g glucose had been added per liter, the progress curves depicting the net enzyme-catalyzed glucose release (Fig. 4) had the typical form of rectangular hyperbola curves for enzymatic reactions, i.e., a relatively fast initial increase followed by a fall-off, which in this case was seen after approximately 6 h from the start of reaction. For the reaction to which no glucose had been added, i.e., ‘0 g/L’, the 6-h point was equivalent to a glucose concentration of 3.6 g/L (net yield was 0.32 g/g; Fig. 4). Similar tendencies were observed for the higher glucose addition levels, although no glucose formation was detected during the first 3 h of hydrolysis with glucose additions of ‘10 g/L’ and ‘20 g/L’ (Fig. 4). In addition, the glucose release was slower when these levels of glucose were added, and the net glucose level formed reached only 1.2 g/L after 6 h (Fig. 4) and the net yield was only 0.11 g/g. With addition of the highest level of glucose, ‘40 g/L’, the net glucose release became negative, probably as a result of transglycosylation

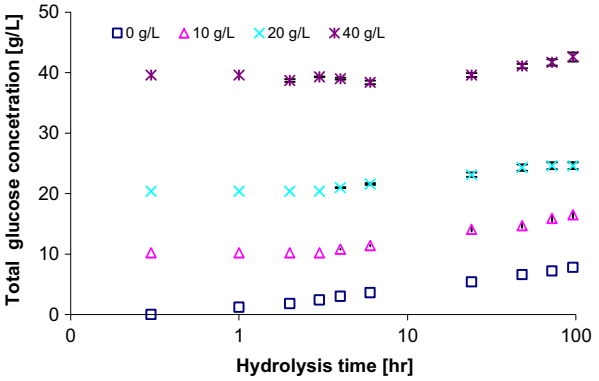

Fig. 3 Reaction progress curves for total glucose concentration in hydrolysis reactors at different glucose addition levels. The reaction was performed at 50 °C, pH 5, 350 rpm, with the commercial cellulase mixture (Celluclast® 1.5L and Novozym® 188, 8 FPU/$g_{dry\ matter}$ and 13 CBU/$g_{dry\ matter}$, respectively), acting on 2% DM (*w*/*w*) hydrothermally pretreated wheat straw of particle size 4 mm in the initial presence of 0–40 g/L of glucose. *x*-axis is given in logarithmic scale

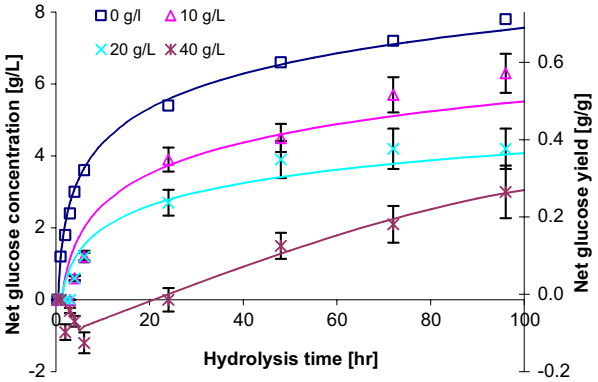

Fig. 4 Net glucose concentration and net glucose yield (grams of formed glucose per gram theoretically available glucose) in the hydrolysis reactors at different initial glucose levels (0–40 g/L). Net glucose concentration was calculated as the difference of total and initially added glucose concentration, while net glucose yield was the ratio of net glucose concentration and maximal theoretically obtainable glucose concentration. The *solids lines*, $G_{\text{fitted}}(t)$, were obtained by fitting the experimental curves, $G_{\text{exp}}(t)$, using soft trend lines. Reaction conditions are given in Fig. 3

reactions (Fig. 1). In our work, glucose was added in appreciable levels (up to 40 g/L), which thus could have directed a transglycosylation equilibrium towards formation of various glucose oligomers. In the light of the increasing requirements for obtaining high glucose yields and concentrations in cellulolytic conversions in relation to bioethanol production, the putative problem of transglycosylation by β-glucosidases during cellulose degradation deserves further attention. For the present reaction, with 40 g/L glucose added, a constant increase in net glucose release was observed only during the extended reaction time (Fig. 4). The final net glucose concentration and net glucose yields decreased considerably with addition of glucose and were 7.8 g/L (0.70 g/g), 6.3 g/L (0.56 g/g), 4.2 g/L (0.38 g/g), and 3.0 g/L (0.27 g/g) after 96 h for the reactions '0 g/L', '10 g/L', '20 g/L', and '40 g/L', respectively (Fig. 4).

Glucose Inhibition of Enzymatic Cellulose Hydrolysis: Effect on Enzyme Efficiency

The efficiency of the enzyme system Celluclast® 1.5 L and Novozym® 188 in releasing glucose from the pretreated wheat straw substrate, represented by the specific cellulase efficiency, calculated as grams glucose formed per gram enzyme system added ($g_{\text{product}}/g_{\text{catalyst}}$), rapidly decreased with glucose addition level (Fig. 5). This specific cellulase efficiency was particularly reduced during the first 6 h of hydrolysis, but for the addition of 40 g/L of glucose, the reduction was 100% or more after 1–24 h of hydrolysis, then 77% after 48 h (1.3 to 0.3 g/g_{enzyme}), 71% after 72 h (1.4 to 0.4 g/g_{enzyme}), and 60% after 96 h (1.5 to 0.6 g/g_{enzyme}; Fig. 5).

For comparison, the specific yield of heterogeneous inorganic catalysts can reach as high as 500 $\text{ton}_{\text{product}}/(\text{h}\cdot\text{m}^3_{\text{catalyst}})$, equivalent to ≈50,000 $g_{\text{product}}/g_{\text{catalyst}}$ during a 96-h reaction (ρ_{catalyst}=1,000 kg/m^3), but typically varies from 0.2 to 1 $\text{ton}_{\text{product}}/(\text{h}\cdot\text{m}^3_{\text{catalyst}})$ or ≈20–100 $g_{\text{product}}/g_{\text{catalyst}}$ as for, e.g., SO_2 oxidation to SO_3 over V_2O_5 and NH_3 synthesis over Fe_2O_3/Al_2O_3 [30]. For enzymatic conversions, the specific enzyme yield can be optimized to reach 10^2–10^4 $g_{\text{product}}/g_{\text{catalyst}}$ which has been reported for, e.g., immobilized enzymes or immobilized cells used for conversion of acrylonitrile to acrylamide [31]. Some of the pharmaceutical biocatalytic processes utilize 0.4–25 $g_{\text{substrate}}/g_{\text{enzyme}}$ [32], which in our work corresponded to ≈0.2–13 $g_{\text{glucose}}/g_{\text{enzyme}}$ based on 100% conversion and 48% by

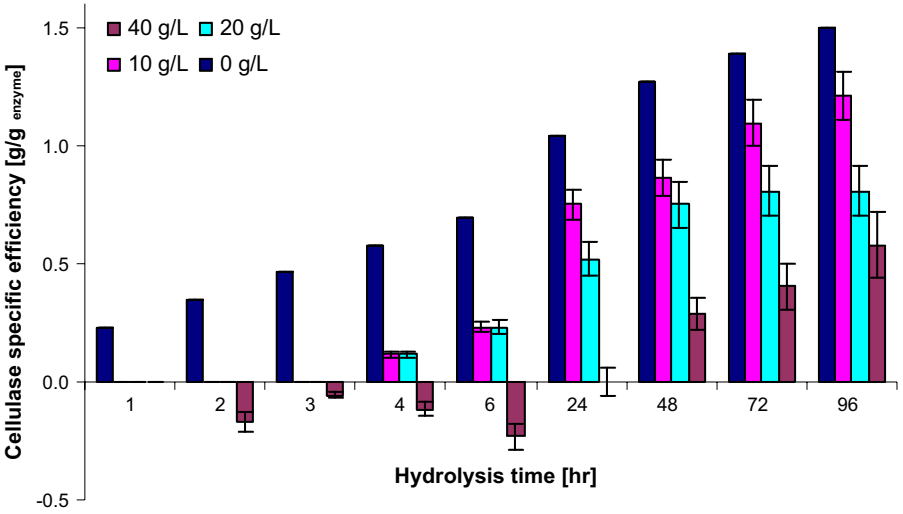

Fig. 5 Specific efficiency (cumulated, in grams formed glucose per gram used enzyme) of commercial cellulase mixture (Celluclast® 1.5 L and Novozym® 188) during hydrolysis of hydrothermally pretreated wheat straw, as function of initially added glucose concentration (0–40 g/L). Specific cellulase efficiency was the ratio of net glucose concentration and enzyme concentration (5.2 g/L). Reaction conditions are given in Fig. 3

weight of cellulose in pretreated straw. Although the specific enzyme efficiency range in our study was probably slightly elevated because of the low substrate dry matter concentration employed, it was in the lower range compared to industrial biocatalytic processes. The enzyme efficiency thus obviously requires further improvement to provide efficient conversion and optimize the use of the enzymes.

Glucose Inhibition of Enzymatic Cellulose Hydrolysis: Effect on Conversion Rates

In order to calculate the time necessary for a given conversion in a batch reactor (or volume in a flow reactor) and to design appropriate reactor systems, it is relevant to evaluate the effects of the glucose inhibition on the rate of reaction as the reaction is progressing. For the highest glucose addition level, '40 g/L', the glucose formation rate, r ($r = \frac{dG}{dt}$), was negative during the first 6 h of reaction, but then rose to a relatively constant value of 25–50 mg/(L·h) (Fig. 6). For the other glucose addition levels, ('0 g/L', '10 g/L', and '20 g/L'), the glucose

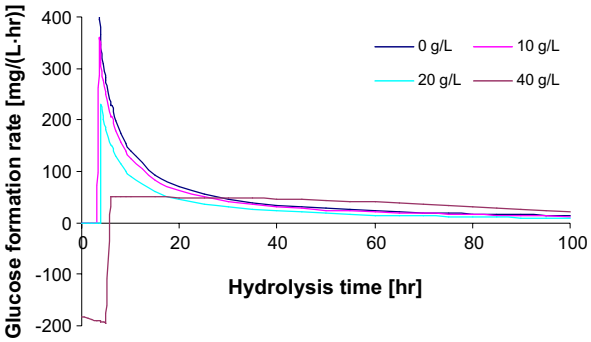

Fig. 6 Glucose formation rate (in constant volume batch reactors) during hydrolysis of the hydrothermally pretreated wheat straw with the Celluclast® 1.5L–Novozym® 188 cellulase system, as a function of initially added glucose concentration (0–40 g/L). The lines representing the rates were calculated as the first derivates of the fitted curves, $G_{\text{fitted}}(t)$. Reaction conditions are given in Fig. 3

formation rate, *r*, decreased rapidly as the enzymatic reaction(s) progressed, irrespective of the glucose addition level (Fig. 6). For the '0 g/L' reaction, the *r* decreased significantly from ≈1,400 to 460 mg/(L·h) between 1 and 3 h of reaction (out of the scale in Fig. 6), but at least glucose formation was observed. Interestingly, for this reaction (0 g/L), the extrapolated rate at 0.1 h was as high as 13.9 g/(L·h). However, after 6 h, when glucose was formed at ≈230, 210, and 150 mg/(L·h) (Fig. 6), the formation rates were relatively constant and similar until the reaction in effect ceased with the rates, having dropped to 15, 13, and 10 mg/(L·h), for '0 g/L','10 g/L', and'20 g/L', respectively (Fig. 6). For these reactions, the differences in *r* were thus significant only during the first 24 h of reaction (statistics not shown).

Glucose inhibition studies were reported previously on commercial enzyme preparations from *T. reesei* (Celluclast 2.0 L type X, CELLULASE GC 123, Laminex, Celluclast) acting on cellulosic substrates such as Solca Floc, dyed cellulose, α-cellulose, or Avicel [10, 17, 18, 22]. It is quite difficult to compare the data from different sources due to the varying reaction conditions (pH, *T*); enzymes composition, activity, and dosage; substrate type, dry matter content; and/or glucose addition level. However, as an example, Xiao et al. [10] found that the commercial cellulase mixture activity (Celluclast® from *T. reesei*, supplemented with Novozym® 188 from *A. niger*) measured after 30 min on 2 DM% (*w*/*v*) Avicel cellulose, was reduced by 55% when 20 g/L of glucose was added. In contrast, we observed a 100% reduction in cellulase efficiency (1–3 h, Fig. 5) when the same level of glucose was added. Since a large enzyme dosage is relatively less affected by inhibition, this difference in glucose inhibition may mainly be due to the large difference in enzyme dosages: Xiao et al. [10] thus used very high enzyme dosages (40 FPU/$g_{cellulose}$, 80 CBU/$g_{cellulose}$), while in the present work, we employed less than half the dosage of FPU and about one third of the cellobiase dosage (17 FPU/$g_{cellulose}$, 27 CBU/$g_{cellulose}$). Hence, the use of relatively low (more realistic) enzyme dosages in the present work brought out the strong significance of the product inhibition.

Glucose Inhibition of Enzymatic Cellulose Hydrolysis: Kinetic Modeling

The multi-enzyme cellulolytic degradation of insoluble cellulose cannot be fully described by classical Michaelis–Menten kinetics [33, 34]. Nevertheless, we evaluated the ability of four simple Michaelis-Menten-based models to predict the effect of glucose addition on the kinetics of the enzymatic degradation of the pretreated wheat straw during extended reaction (96 h; Table 1). The fitting of the progress curves to the presented models was not intended to identify the exact type of mechanisms underlying the cellulase inhibition by glucose, but was rather employed to obtain a simple tool that would allow a prediction of the degree of inhibition on the hydrolysis, specifically with respect to the net glucose formation rate and glucose concentration, and which in turn might be used as an initial base for selection of reactor design strategies and scale-up.

Surprisingly, even being oversimplified, the models gave a reasonably good prediction of the influence of glucose addition on the extent of hydrolysis—but did not, as expected, properly predict the progress of the '0 g/L' reaction (Fig. 7). From Fig. 7, it is evident, however, that all the models had a considerable deviation from the experimental data.

The difference in the prediction of the reaction progress during the early vs. the late progress stages of the reaction was probably due to the inability of these models to allow for the changes in (rate of) substrate formation for the β-glucosidase. This may be a result of a faster cellobiose (and cellulo-oligosaccharide) formation rate during the initial reaction period when more substrate attack points are presumably available for the endoglucanases

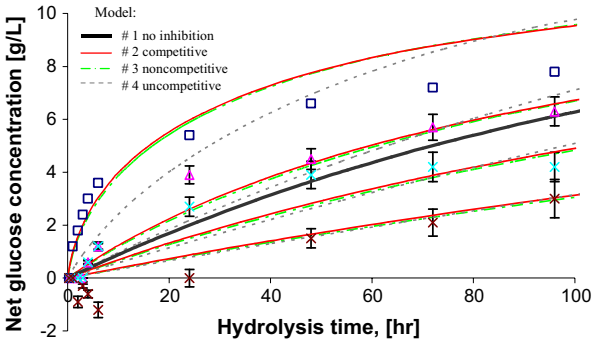

Fig. 7 Simple inhibition models for hydrolysis of pre-treated wheat straw by commercial cellulase mixture (Celluclast® 1.5L and Novozym® 188) in the presence of initially added glucose (0–40 g/L) glucose addition graphic tags as in Figs. 3 and 4. Model identification results. Selected results of parameter optimization. Parameter values are average with 95% confidence intervals. The optimal parameter values: model 1 (k_{cat}= 8.4 h^{-1}, K_M=10 mM, K_{IG}=0 mM); model 2 (k_{cat}=14 h^{-1}, K_M=0.9 mM, K_{IG}=5 mM); model 3 (k_{cat}=12 h^{-1}, K_M=0.9 mM, K_{IG}=6.4 mM); and model 4 (k_{cat}=9.9 h^{-1}, K_M=3.1 mM, K_{IG}=1 mM). Constants in the models: S_0=0.136 mM, E_0=0.01 mM, n=450. Initial parameter values: k_{cat}=10 h^{-1}, K_M=1 mM, K_{IG}=10 mM

and the cellobiohydrolases [3]. The lack of prediction ability for the highest glucose addition level (40 g/L) during 0–24 h may be a result of that none of the models included consideration of reversion reactions (i.e., the likely transglycosylation) taking place at this high glucose addition level. The uncompetitive inhibition model (model no. 4, Table 1) generally predicted a lower glucose release than the competitive or non-competitive models (Fig. 7).

The modeled values for the inhibition constant for glucose (K_{IG}) ranged from 1 to 6.4 mM, equivalent to 0.18–1.2 g glucose per liter. This range was significantly lower than the K_{IG} values previously reported for *T. reesei* cellulase mixtures—which have ranged from 12 to 319 g/L [6, 17, 23, 35]. However, the K_{IG} values were in good accordance with the available values for glucose inhibition of β-glucosidase from *A. niger*, which are in the range 0.3–0.5 g/L [23, 36]. This latter accordance indicated that our models might in fact mainly have quantified the glucose inhibition of the *A. niger* β-glucosidase in the employed enzyme system (see discussion further below).

Assessment of the Model Predictions

The parameters k_{cat}, K_M, and K_{IG} had very large confidence intervals which, in most cases, exceeded the value of the parameter itself (data not shown). Obviously, because of the Michaelis–Menten equation origin, the k_{cat} and K_M were highly correlated, with correlation coefficients of 0.99–1, while k_{cat} and K_{IG} (0.63–0.88, absolute values) and K_M and K_{IG} (0.49–0.90, absolute values) were less correlated, at least for models 2 (competitive inhibition) and 3 (non-competitive inhibition). The relatively low quality of the parameter estimations did, however, not significantly impact on the model uncertainty (data not shown). This result was probably due to the high correlation of the k_{cat} and K_M parameter in effect compensating for the high error on the parameter estimates.

The models presented in this work mainly described the influence of product inhibition by glucose on the hydrolysis rate (Table 1), and many simplifying assumptions were thus made. In addition, k_{cat}, and in turn K_M, may not be constant during extended cellulose hydrolysis. That k_{cat} and K_M are constant during the course of hydrolysis is obviously one of the cornerstones of Michaelis–Menten kinetics, as evidenced by the reaction rate expressions (Table 1). Hence, the Michaelis-Menten-based models could obviously not

fully describe the complex, multi-enzyme-catalyzed cellulose degradation. Rather, the models may in fact mainly have fitted the glucose inhibition of the β-glucosidase activity, since this activity is known to be directly product inhibited by glucose and is expected to largely follow Michaelis–Menten kinetics because the major substrate for the reaction, cellobiose, is soluble (Fig. 1). In addition, the initial presence of glucose in relatively high concentration [in a reaction mixture with only 2% DM (*w*/*w*) substrate] may have brought the product inhibition effect forward at the expense of the other important rate-determining factors influencing enzymatic cellulose degradation—a situation which was desirable in this work. The product inhibition of β-glucosidase by glucose has been reported to take place via a competitive inhibition mechanism [3, 37, 38]. However, in the present work, the non-competitive inhibition model seemed to fit the data the best. This finding does not exclude that the true product inhibition of β-glucosidase (and cellulases) by glucose did really take place via a competitive inhibition mechanism because the non-competitive inhibition actually incorporates competitive inhibition (i.e., a direct reaction between the inhibitor and the enzyme). However, the non-competitive mechanism also includes the possible reaction between the inhibitor and the enzyme–substrate complex (Table 1). In the hydrolysis rate expression, these reactions are accounted for by an interaction between the inhibitor (in this case G) and the dissociation constant for the inhibitor and the enzyme (K_{IG}) as well as for the inhibitor and the enzyme–substrate complex (K_{IG}'; Table 1). For simplicity, K_{IG} and K_{IG}' were assumed to be equal and described as K_{IG} (Table 1). In effect, this resulted in an expression which included an interaction of the inhibitor with both the substrate concentration (S) and the enzyme–cellulose complex dissociation constant (K_M; Table 1). Hence, as the only one amongst the models, the non-competitive model incorporated an inhibitory effect on top of the direct competitive product inhibition by glucose. It is likely that the inclusion of such an extra inhibitory effect may have partly accounted for some of the complex influence from the multi-enzymatic cellulose degradation rather than defining a true non-competitive inhibition mechanism.

A preliminary iteration of the models with the data signified that for both the competitive inhibition model (model 2, Table 1) and the non-competitive model (model 3, Table 1), the best fits were obtained with a k_{cat} value ≈10 h^{-1}, a K_M value ≈1 mM, and a K_{IG}≈10 mM (data not shown). It would be interesting if a K_M value for the cellulolytic degradation of the cellulose in the substrate could actually be determined experimentally. However, this is inherently impossible with multi-enzymatic degradation of cellulose in genuine lignocellulosic substrates because S is inherently unknown. Secondly, as mentioned above, one of the main reasons for the enzymatic degradation of lignocellulosic substrates not to follow Michaelis–Menten kinetics may be that for each individual enzyme reaction, the k_{cat}, and in turn K_M, may not be constant during the course of the cellulose hydrolysis and may vary in an unpredictable way because of the interaction effects among the enzymatic reactions, e.g., endoglucanase activity gives more substrate ends for cellobiohydrolase attack, etc.

In the present work, the main objective was to investigate and model the effect of glucose inhibition on the overall reaction rate of the multi-enzyme-catalyzed degradation of cellulose in lignocellulose isolated from other rate- and yield-limiting factors. Among the latter, one of the most important factors is the accessible surface area of the lignocellulosic particles. This area depends mainly on the (initial) particle size and pretreatment. We have recently shown that enzyme-catalyzed glucose release from finely ground wet oxidized wheat straw particles (diameter 53–149 μm) took place at a higher rate and reached higher yields than those obtained with reference straw samples of 2–4 cm [39]. However, the true effect of decreasing substrate particle size, or rather an

increased accessible surface area, may only be apparent if the glucose product is removed. The experimental and mathematical model validation of this assumption is among our future research priorities.

Effect of In Situ Glucose Removal During Enzymatic Hydrolysis

Removal of glucose during the enzymatic hydrolysis of the pretreated straw was evaluated by three different methods (Fig. 2): (1) buffer replenishment via filtration of the hydrolysate liquid, (2) buffer and enzyme replenishment via filtration of the hydrolysate liquid, and (3) dialysis, with the glucose removal initiated after 24 h of reaction (Fig. 8).

With all three methods, the glucose removal resulted in substantial decreases of the glucose concentration, from 4.5–4.9 to 0.28–2.0 g/L (Fig. 9). The reductions in glucose concentrations were equivalent to reductions of 59%, 65%, and 94%, for methods 1, 2, and 3, respectively, and was highest for the in situ membrane dialysis method (Fig. 9). The incomplete removal of glucose with methods 1 and 2 was probably due to the relatively short liquid filtration process (15 min by intermission) that furthermore might have removed only the portion which was fast to filter (≈30 g).

The slopes of the glucose formation rates of the reaction progress curves changed to different extents for the three removal methods (Fig. 9). For the removal with filtration and replenishment of fresh buffer (method 1), the glucose formation slope dropped from 100 mg/(L·h) (average taken at 6–24 h, Fig. 9) to only 4 mg/(L·h) (average 24–48 h), and afterward rose to 24 mg/(L·h) (average 48–72 h). The reduction was probably due to the simultaneous dilution and removal of the enzymes present in the reaction mixture because buffer, enzymes, and glucose were removed and only buffer was returned. Obviously, although product inhibition was relieved, this effect did not suffice to overcome the loss of enzymes. When both enzymes and buffer were replaced by a fresh portion (method 2), the enzyme concentration was kept at the same level, which, together with glucose removal, resulted in a recovery of the slope, namely 88 mg/(L·h) at 6–24 h and 90 mg/(L·h) at 24–48 h (Fig. 9). It thus seemed that the supplementation of fresh enzymes maintained the glucose formation rate (e.g., slope) at the same level as before the removal (Fig. 9). However, after the glucose concentration reached 3.5 g/L, the slope fell to 28 mg/(L·h).

When removing the glucose by dialysis during the cellulolytic hydrolysis reaction (from 24–48 h, method 3; Fig. 9), the glucose formation rate decreased from 92 mg/(L·h) (from

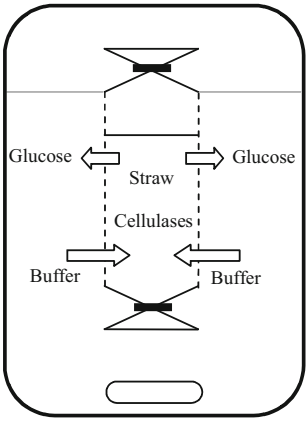

Fig. 8 Stylized representation of a membrane reactor for enzymatic degradation of wheat straw with in situ product removal. Pretreated wheat straw was hydrolyzed inside the dialysis membrane. Glucose diffused through the membrane (1 kDa cut-off) and there was a reverse flux of solvent (1 M citrate buffer) from the dialysate solution

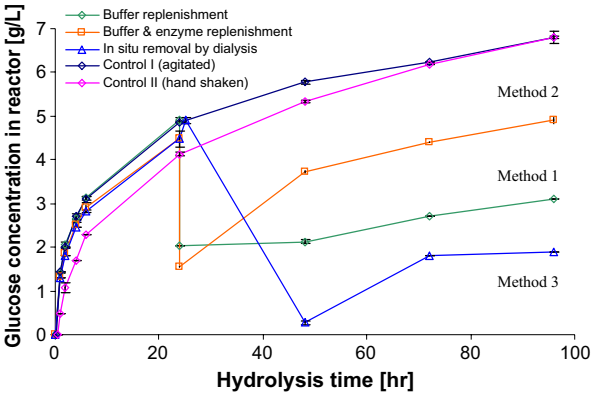

Fig. 9 Glucose concentration in hydrolysis reactor during removal of glucose by: (1) filtration and replenishment of fresh buffer; (2) filtration and replenishment of fresh buffer and enzymes; and (3) dialysis membrane (in situ). The reaction was performed at 50 °C, pH 5, 350 rpm, with Celluclast® 1.5L and Novozym® 188 (8 FPU/$g_{dry\ matter}$ and 13 CBU/$g_{dry\ matter}$, respectively) on 2% DM (*w*/*w*) hydrothermally pretreated wheat straw. The reaction mixture was not stirred during filtration (for 15 min) or dialysis (for 24 h). The dialysis membrane cutoff was 1 kDa. The two controls (no glucose removal) had the same hydrolysis conditions. For control II, the reaction mixture was intermittently hand-shaken

6–24 h) to 64 mg/(L·h) (48–72 h). However, although the glucose formation rate was reduced by 30%, this rate was the highest for this reaction period amongst the three removal methods applied, and it was significantly higher than the rate of the control(s) from which no glucose had been removed. For control I, the glucose formation rate was 38 and 17 mg/(L·h) (24–48 and 48–72 h, respectively; Fig. 9), while for control II, it was 50 and 38 mg/(L·h) (24–48 and 48–72 h, respectively).

We ascribe this regaining of a relatively high glucose production rate to be a result of alleviation of the product inhibition, as corroborated by the very low glucose concentration in the reactor. The low glucose concentration was a direct result of the dialytic glucose removal in situ (retaining the enzymes with the substrate), but the reduction of the glucose concentration was also enhanced as a result of penetration of the dialysate buffer into the hydrolysis reactor (Fig. 8). This flow was an unavoidable consequence of the difference in the chemical potential across the dialysis membrane, including osmotic pressure, caused by the presence of the wheat straw substrate in the reactor.

In independent tests of membrane performance with 2% (*w*/*w*) DM pretreated wheat straw, this dialysate flux into the reactor decreased from 2.0 to 0.5 mg/(min·cm^2) during 2 h from the start of the hydrolysis (data not shown). Thus, the dialysate flux into the dialysis membrane reactor might have diluted the glucose concentration and in this way contributed to relieve the glucose product inhibition. Furthermore, the glucose concentration in the dialysate solution during the removal (method 3) changed from 0 to a final concentration of 0.045 g/L—the final concentration being relatively low due to the large amount of buffer employed as dialysate solution. The low glucose concentration in the dialysate indicated that the dialysis driving force, i.e., the difference in glucose levels in the reactor and the dialysate, could have remained at a significant level, the lowest being from 0.28 to 0.045 g/L. Thus, it is very likely that the dialysis membrane would be able to reduce the glucose concentration in a hydrolysis reactor and relieve the inhibition even without any solvent penetration. Moreover, apart from reducing the dialysis driving force, the solvent penetration must have decreased the substrate and enzyme concentration, which in turn may

have compensated for the positive effect of the solvent flux on the glucose formation rate. Thus, the benefits of dialysis removal might be better without solvent influx and dilution.

The integrity of the membrane towards the cellulase activity was tested using a cellulase addition level of ≈5 g/L with 2% (*w*/*w*) pretreated wheat straw. No leaking from the membrane was observed. Furthermore, the dialysis membrane was submitted for 2 h to the pure cellulase mixture (50 mL, Celluclast® 1.5 L+ Novozym® 188, in ratio 4:1) at 50 °C, and no mechanical ruptures were seen. To additionally reduce the potential influence of cellulase activity on the dialysis membrane, simultaneous removal and hydrolysis (24–48 h) was performed at room temperature.

Previously, in a reaction mixture containing 2% DM (*w*/*w*) hydrothermally pretreated wheat straw (50 °C, pH 5), and a commercial cellulase mixture (Celluclast® 1.5 L and Novozym® 188, 8 FPU/$g_{dry\ matter}$ and 13 CBU/$g_{dry\ matter}$, respectively), the cellobiose concentration after 24 h was never higher than 0.04–0.06 g/L (data not shown). Thus, if any cellobiose would be removed from the reactor during the dialysis, this removal would in any case impart an infinitesimal effect on the reaction rate. Removal of glucose by in situ dialysis (method 3) thus resulted in the highest glucose yield, 0.94 g/g after 96 h of hydrolysis. This maximal yield was reached after approximately 72 h of reaction, and at this time point, this yield was ≈25% higher than that of the control(s) (Fig. 10).

Glucose Removal Modeling

The increase in the glucose yield obtained after the glucose removal by dialysis was also found to fit the non-competitive Michaelis–Menten model reasonably well (Fig. 11). This indicated that the non-competitive model (model 3, Table 1) might prove useful for estimating reaction times for cellulolytic conversions and for dimensioning and scale-up of lignocellulose hydrolysis reactors.

Conclusions

The data confirmed that glucose exerts a dose-dependent significant inhibitory effect on the cellulolytic conversion of lignocellulose, in this case pretreated wheat straw catalytically hydrolyzed by the Celluclast®–Novozym® 188 cellulase system. The glucose-induced inhibition of the glucose production with time was modeled surprisingly well by means of relatively simple Michaelis–Menten models, especially the model that incorporated the non-

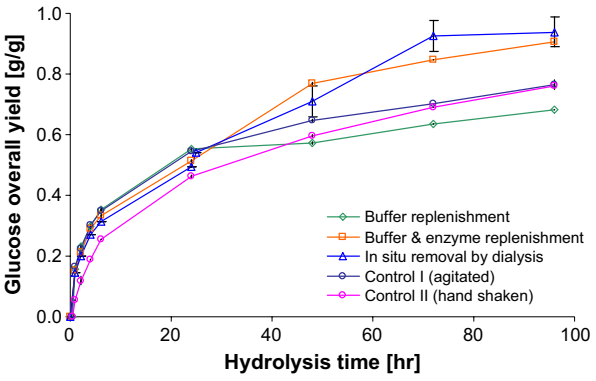

Fig. 10 Glucose yield from a hydrolysis reactor during removal of glucose by: (1) filtration and replenishment of fresh buffer; (2) filtration and replenishment of fresh buffer and enzymes; and (3) dialysis membrane (in situ). Reaction conditions are given in Fig. 9

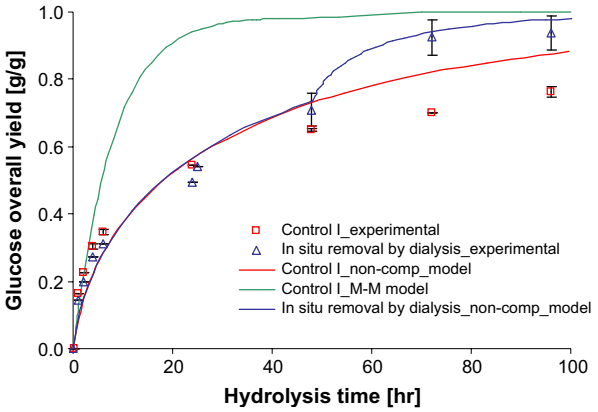

Fig. 11 Comparison of experimental and modeling results for in situ removal of glucose by dialysis and control I. Reaction conditions are given in Fig. 9. The parameters of the model (no. 3, non-competitive inhibition) were optimal (k_{cat}=12 h^{-1}, K_M=0.9 mM, and K_{IG}=6.4 mM), determined using glucose addition studies. For the non-competitive model for in situ removal by dialysis, it was assumed that present glucose was removed at 48 h (only 0.28 g/L=1.6 mM glucose left, Fig. 9). Just before removal, G=6.6 g/L=37 mM ($S=S_0-cG$). Just after the removal, the reaction proceeded with conditions: G_0=1.6 mM, k_{cat}=12 h^{-1}, K_M= 0.9 mM, and K_{IG}=6.4 mM. The solvent flux into the membrane reactor was neglected in the models. Model 1 parameters (no inhibition) for control I were k_{cat}=12 h^{-1} and K_M=0.9 mM, while for model 3, the parameters were the same as for the dialysis removal

competitive mechanism. The identification of a relatively simple kinetic expression for the complex multiple-enzyme-catalyzed conversion allows for prediction of glucose yields after prolonged reactions and is particularly relevant in relation to reactor design (scaling) of lignocellulosic conversion processes.

Continuous removal of glucose by in situ dialysis (from 24–48 h of reaction) was a promising method for alleviating the product inhibition during enzymatic hydrolysis of lignocellulose. Although dialysis may not be feasible for large-scale applications, the finding provides a strong impetus for the introduction of product removal in hydrolysis reactor design to obtain enhanced cellulose degradation rates, shorter reaction times, higher yields, and more efficient enzyme use. The apparent reversion reaction that was seen at high glucose levels (possibly due to transglycosylation reactions) further emphasizes the need for design of lignocellulose hydrolysis reactors incorporating in situ glucose removal.

Nomenclature

c	reciprocal value of n
E_0	total initial cellulose concentration (M)
E	free enzyme concentration (M)
EG	enzyme–glucose complex concentration (M)
ES	enzyme–cellulose complex concentration (M)
ESG	enzyme–cellulose–glucose complex concentration (M)
G_0	initial glucose concentration (M)
k_{cat}	apparent cellulase turn-over number (s^{-1})
K_M	apparent Michaelis constant (M)
K_{IG}	enzyme–glucose complex dissociation constant (M)
K_{IG}'	enzyme–cellulose–glucose complex dissociation constant (M)
k_1	forward rate constant for enzyme–cellulose complex formation (M^{-1} s^{-1})

k_{-1} reverse rate constant for enzyme–cellulose complex formation (s^{-1})
k_2 rate constant for formation of glucose (=k_{cat}) (s^{-1})
k_{G1} forward rate constant for enzyme–glucose and enzyme–cellulose–glucose complex formation (M^{-1} s^{-1})
k_{G-1} reverse rate constant for enzyme–glucose and enzyme–cellulose–glucose complex formation (s^{-1})
n number of glucose units in molecule of cellulose from pre-treated wheat straw
r glucose formation rate in a constant volume batch reactor (M s^{-1})
S_0 initial concentration of cellulose from pre-treated wheat straw (M)
S concentration of cellulose from pre-treated wheat straw (M)
t hydrolysis time (s)
T temperature (°C)
v cellulose consumption rate in a constant volume batch reactor (reaction rate) (M s^{-1})

Acknowledgment The authors thank Novozymes A/S for providing the enzymes. Dong Energy A/S is acknowledged for supplying the pretreated wheat straw. Dr. Gürkan Sin, Department of Chemical and Biochemical Engineering, Technical University of Denmark, is acknowledged for his help with the numerical simulations. This work is part of the CHEC (Combustion and Harmful Emission Control) Research Center funded a.o. by the Technical University of Denmark, the Danish Technical Research Council, the European Union, the Nordic Energy Research, Dong Energy A/S, Vattenfall A.B., F L Smidth A/S, and Public Service Obligation funds from Energinet.dk and the Danish Energy Research program.

References

1. Merino, S., & Cherry, J. (2007). *Advances in Biochemical Engineering/Biotechnology*, *108*, 95–120. doi:10.1007/10_2007_066.
2. Palonen, H., Tjerneld, F., Zacchi, G., & Tenkanen, M. (2004). *Journal of Biotechnology*, *107*, 65–72. doi:10.1016/j.jbiotec.2003.09.011.
3. Zhang, Y.-I. P., & Lynd, L. R. (2004). *Biotechnology and Bioengineering*, *88*, 797–824. doi:10.1002/bit.20282.
4. Rosgaard, L., Pedersen, S., Langston, J., Akerhielm, D., Cherry, J. R., & Meyer, A. S. (2007a). *Biotechnology Progress*, *23*, 1270–1276. doi:10.1021/bp070329p.
5. Shoemaker, S., Watt, K., Tsitovsky, G., & Cox, R. (1983). *Biotechnology*, *1*, 687–690. doi:10.1038/nbt1083-687.
6. Tolan, J. S., & Foody, B. (1999). Cellulase from submerged fermentation. In *Recent progress in bioconversion of lignocellulosics*. Berlin: Springer, Advances in Biochemical Engineering/Biotechnology Book Series, vol. 65, pp. 41–67.
7. García-Aparicio, M. P., Ballesteros, I., González, A., Oliva, J. M., Ballesteros, M., & Negro, M. J. (2006). *Applied Biochemistry and Biotechnology*, *129–132*, 278–288. doi:10.1385/ABAB:129:1:278.
8. Rosgaard, L., Pedersen, S., & Meyer, A. S. (2007b). *Applied Biochemistry and Biotechnology*, *143*, 284–296. doi:10.1007/s12010-007-8001-6.
9. Rosgaard, L., Andric, P., Dam-Johansen, K., Pedersen, S., & Meyer, A. S. (2007c). *Applied Biochemistry and Biotechnology*, *143*, 27–40. doi:10.1007/s12010-007-0028-1.
10. Xiao, Z., Zhang, X., Gregg, D. J., & Saddler, J. N. (2004). *Applied Biochemistry and Biotechnology*, *113–116*, 1115–1126. doi:10.1385/ABAB:115:1-3:1115.
11. Watanabe, T., Sato, T., Yoshioka, S., Koshijma, T., & Kuwahara, M. (1992). *European Journal of Biochemistry*, *209*, 651–659. doi:10.1111/j.1432-1033.1992.tb17332.x.
12. Schmid, G., & Wandrey, C. (1989). *Biotechnology and Bioengineering*, *33*, 1445–1460. doi:10.1002/bit.260331112.
13. Gan, Q., Allen, S. J., & Taylor, G. (2003). *Process Biochemistry*, *38*, 1003–1018. doi:10.1016/S0032-9592(02)00220-0.
14. Gusakov, A. V., Sinitsyn, A. P., & Klyosov, A. A. (1987). *Biotechnology and Bioengineering*, *29*, 906–910. doi:10.1002/bit.260290715.
15. Asenjo, J. (1983). *Biotechnology and Bioengineering*, *25*, 3185–3190.

16. Gruno, M., Väljamäe, P., Pettersson, G., & Johansson, G. (2004). *Biotechnology and Bioengineering*, *86*, 503–511. doi:10.1002/bit.10838.
17. Philippidis, G. P., Smith, T. K., & Wyman, C. E. (1993). *Biotechnology and Bioengineering*, *41*, 846–853. doi:10.1002/bit.260410903.
18. Tjerneld, F., Persson, I., Albertsson, P., & Hahn-Hägerdal, B. (1985). *Biotechnology and Bioengineering*, *27*, 1044–1050. doi:10.1002/bit.260270716.
19. Belafi-Bako, K., Koutinas, A., Nemestóthy, N., Gubicza, L., & Webb, C. (2006). *Enzyme and Microbial Technology*, *38*, 155–161. doi:10.1016/j.enzmictec.2005.05.012.
20. Gan, Q., Allen, S. J., & Taylor, G. (2002). *Biochemical Engineering Journal*, *12*, 223–229. doi:10.1016/S1369-703X(02)00072-4.
21. Yang, S., Ding, W., & Chen, H. (2006). *Process Biochemistry*, *41*, 721–725. doi:10.1016/j.procbio.2005.08.002.
22. Holtzapple, M., Cognata, M., Shu, Y., & Hendrickson, C. (1990). *Biotechnology and Bioengineering*, *36*, 275–287. doi:10.1002/bit.260360310.
23. Oh, K.-K., Kim, S.-W., Jeong, Y.-S., & Hong, S.-I. (2000). *Applied Biochemistry and Biotechnology*, *89*, 15–30. doi:10.1385/ABAB:89:1:15.
24. Frenneson, I., Trägårdh, G., & Hahn-Hägerdal, B. (1985). *Biotechnology and Bioengineering*, *27*, 1328–1334. doi:10.1002/bit.260270909.
25. Adey, B., & Baker, J.(1996). NREL Laboratory analytical procedure 006. Retrieved May 2, 2006 from http://devafdc.nrel.gov/pdfs/4689.pdf.
26. Sluiter, A. (2006). Laboratory Analytical Procedure 002. Determination of structural carbohydrate and lignin in biomass. Retrieved May 2, 2006 from http://www.nrel.gov/biomass/analytical_procedures.html.
27. Keller, F. A., Hamilton, J. E., & Nguyen, Q. A. (2003). *Applied Biochemistry and Biotechnology*, *105–108*, 27–41. doi:10.1385/ABAB:105:1-3:27.
28. Arnous, A., & Meyer, A. S. (2008). *Food and Bioproducts Processing*, *86*, 79–86.
29. Sin, G., Ödman, P., Petersen, N., Lantz, A. E., & Gernaey, K. V. (2008). *Biotechnology and Bioengineering*, *101*, 153–171. doi:10.1002/bit.21869.
30. Baerns, M., Hofmann, H., & Renken, A.(1999). Chemische reaktionstechnik, Lehrbuch der Technischen Chemie, 3. durchgesehene Auflage, Band 1, Wiley-VCH, p. 45.
31. Thomas, S. M., DiCosimo, R., & Nagarajan, V. (2002). *Trends in Biotechnology*, *20*, 238–242. doi:10.1016/S0167-7799(02)01935-2.
32. Straathof, A. J. J., Panke, S., & Schmid, A. (2002). *Current Opinion in Biotechnology*, *13*, 548–556. doi:10.1016/S0958-1669(02)00360-9.
33. Fan, L. T., & Lee, Y. - H. (1983). *Biotechnology and Bioengineering*, *25*, 939–966. doi:10.1002/bit.260251115.
34. Wald, S., Wilke, C. R., & Blanch, H. W. (1984). *Biotechnology and Bioengineering*, *24*, 221–230. doi:10.1002/bit.260260305.
35. Holtzapple, M. T., Caram, H. S., & Humphrey, A. E. (1984). *Biotechnology and Bioengineering*, *24*, 753–757. doi:10.1002/bit.260260719.
36. Dekker, R. F. H. (1996). *Biotechnology and Bioengineering*, *28*, 1438–1442. doi:10.1002/bit.260280918.
37. Lee, Y. - H., & Fan, L. T. (1983). *Biotechnology and Bioengineering*, *25*, 939–966. doi:10.1002/bit.260250406.
38. Gusakov, A. V., & Sinitsyn, A. P. (1992). *Biotechnology and Bioengineering*, *40*, 663–671. doi:10.1002/bit.260400604.
39. Pedersen, M., & Meyer, A. S. (2009). *Biotechnology Progress* (in press).
40. Huang, X., & Penner, M. H. (1991). *Journal of Agricultural and Food Chemistry*, *39*, 2096–2100. doi:10.1021/jf00011a042.
41. Väljamäe, P., Petterson, G., & Johansson, G. (2001). *European Journal of Biochemistry*, *268*, 4520–4526. doi:10.1046/j.1432-1327.2001.02377.x.